- Re-engineering protein interfaces yields copper-inducible ferritin cage assembly
  Huard, D. J. E.; Kane, K. M.; Tezcan, F. A. *Nature Chem. Biol.* **2013**, *9*, 169-176.
  Abstract:

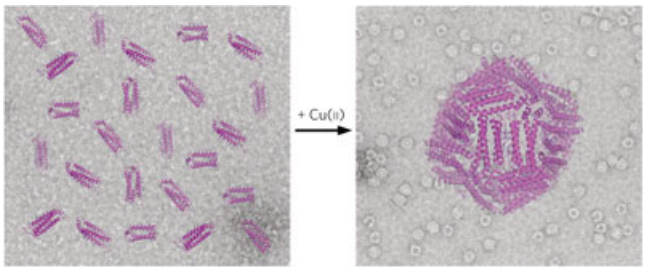

The ability to chemically control protein-protein interactions would allow the interrogation of dynamic cellular processes and lead to a better understanding and exploitation of self-assembling protein architectures. Here we introduce a new engineering strategy—reverse metal-templated interface redesign (rMeTIR)—that transforms a natural protein-protein interface into one that only engages in selective response to a metal ion. We have applied rMeTIR to render the self-assembly of the cage-like protein ferritin controllable by divalent copper binding, which has allowed the study of the structure and stability of the isolated ferritin monomer, the demonstration of the primary role of conserved hydrogen-bonding interactions in providing geometric specificity for cage assembly and the uniform chemical modification of the cage interior under physiological conditions. Notably, copper acts as a structural template for ferritin assembly in a manner that is highly reminiscent of RNA sequences that template virus capsid formation.

- Structure and function of a unique pore-forming protein from a pathogenic acanthamoeba
  Michalek, M.; Sönnichsen, F. D.; Wechselberger, R.; Dingley, A. J.; Hung, C.-W.; Kopp, A.; Wienk, H.; Simanski, M.; Herbst, R.; Lorenzen, I.; Marciano-Cabral, F.; Gelhaus, C.; Gutsmann, T.; Tholey, A.; Grötzinger, J.; Leippe, M. *Nature Chem. Biol.* **2013**, *9*, 37-42.
  Abstract:

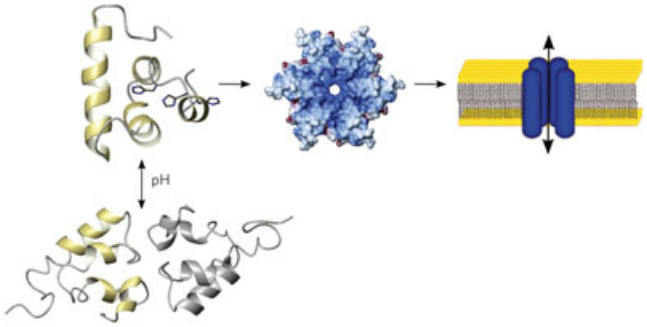

Human pathogens often produce soluble protein toxins that generate pores inside membranes, resulting in the death of target cells and tissue damage. In pathogenic amoebae, this has been exemplified with amoebapores of the enteric protozoan parasite *Entamoeba histolytica.* Here we characterize acanthaporin, to our knowledge the first pore-forming toxin to be described from acanthamoebae, which are free-living, bacteria-feeding, unicellular organisms that are opportunistic pathogens of increasing importance and cause severe and often fatal diseases. We isolated acanthaporin from extracts of virulent *Acanthamoeba culbertsoni* by tracking its pore-forming activity, molecularly cloned the gene of its precursor and recombinantly expressed the mature protein in bacteria. Acanthaporin was cytotoxic for human neuronal cells and exerted antimicrobial activity against a variety of bacterial strains by permeabilizing their membranes. The tertiary structures of acanthaporin's active monomeric form and inactive dimeric form, both solved by NMR

spectroscopy, revealed a currently unknown protein fold and a pH-dependent trigger mechanism of activation.

- Tactile-Feedback Stabilized Molecular Junctions for the Measurement of Molecular Conductance
  Chen, I.-W. P.; Tseng, W.-H.; Gu, M.-W.; Su, L.-C.; Hsu, C.-H.; Chang, W.-H.; Chen, C.-H. *Angew. Chem. Int. Ed.* **2013**, *52*, 2449-2453.
  Abstract:

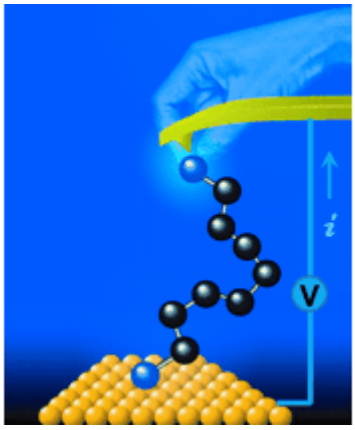

Handling the (AFM) tip: The duration of stable molecular junctions was prolonged using a tactile feedback method in which the operator can sense the force of the AFM tip on the sample surface (see picture). The movement of the tip is adjusted accordingly, maintaining a more consistent current (*i*) and voltage (V), instead of having the tip move at a constant preset speed, as in the conventional setup.

- Hydrodynamically Driven Self-Assembly of Giant Vesicles of Metal Nanoparticles for Remote-Controlled Release
  He, J.; Wei, Z.; Wang, L.; Tomova, Z.; Babu, T.; Wang, C.; Han, X.; Fourkas, J. T.; Nie, Z. *Angew. Chem. Int. Ed.* **2013**, *52* 2463-2468.
  Abstract:

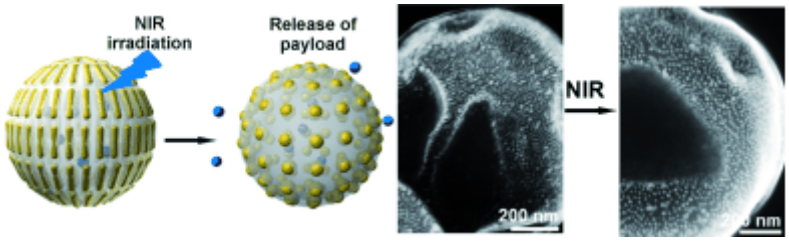

The hydrodynamics of laminar flow in a microfluidic device has been used to control the continuous self-assembly of gold nanoparticles (NPs) tethered with amphiphilic block copolymers. Spherical micelles, giant vesicles (500 nm–2.0 µm), or disk-like micelles could be formed by varying the flow rates of fluids. Such vesicles can release encapsulated hydrophilic species by using near-IR light (see picture).

- A Structured Monodisperse PEG for the Effective Suppression of Protein Aggregation
  Muraoka, T.; Adachi, K.; Ui, M.; Kawasaki, S.; Sadhukhan, N.; Obara, H.; Tochio, H.; Shirakawa, M.; Kinbara, K. *Angew. Chem. Int. Ed.* **2013**, *52*, 2430–2434.
  Abstract:

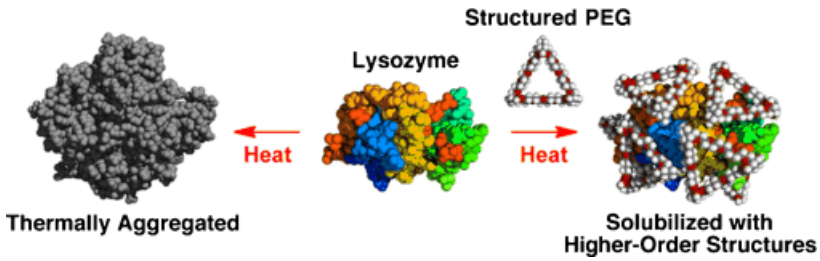

Part of the solution: A PEG with a discrete triangular structure exhibits hydrophilicity/hydrophobicity switching upon increasing temperatures, and suppresses the thermal aggregation of lysozyme to retain nearly 80 % of the enzymatic activity. CD and NMR spectroscopic studies revealed that, with the structured PEG, the higher-order structures of lysozyme persist at high temperature, and the native conformation is recovered after cooling.

- Large-Scale Hierarchically Structured Conjugated Polymer Assemblies with Enhanced Electrical Conductivity
  Han, W.; He, M.; Byun, M.; Li, B.; Lin, Z. *Angew. Chem. Int. Ed.* **2013**, *52*, 2564–2568.
  Abstract:

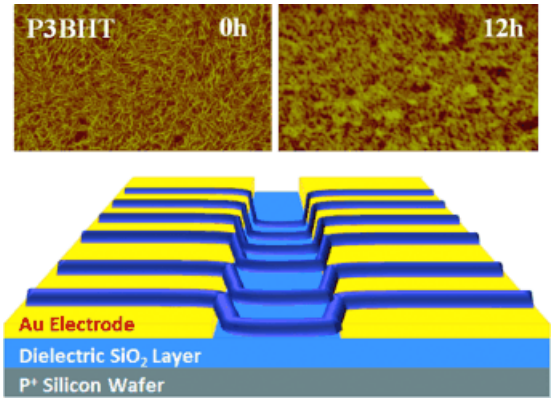

Stripes on a plane: A set of highly ordered microscopic stripes (purple; see scheme) were produced over a large area by using controlled evaporative self-assembly in a cylinder-on-Si geometry of conjugated homopolymers or all-conjugated diblock copolymer (P3BHT). The crystallinity of the as-prepared assemblies of P3BHT was greatly improved following chloroform vapor annealing, resulting in a fourfold increase in electrical conductivity.

- The Smartest Materials: The Future of Nanoelectronics in Medicine
  Cohen-Karni, T.; Langer, R.; Kohane, D. S. *ACS Nano* **2012**, *6,* 6541–6545.
  Abstract:

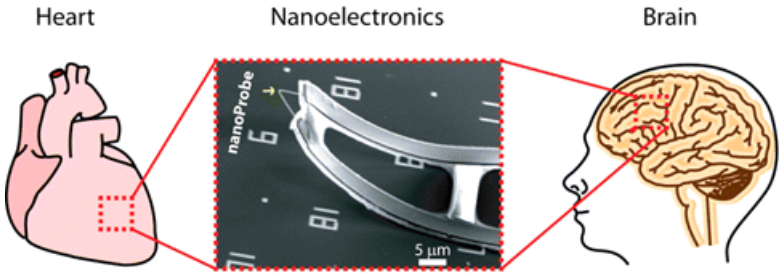

Electronics have become central to many aspects of biomedicine, ranging from fundamental biophysical studies of excitable tissues to medical monitoring and electronic implants to restore limb movement. The development of new materials and approaches is needed to enable enhanced tissue integration, interrogation, and stimulation and other functionalities. Nanoscale materials offer many

avenues for progress in this respect. New classes of molecular-scale bioelectronic interfaces can be constructed using either one-dimensional nanostructures, such as nanowires and nanotubes, or two-dimensional nanostructures, such as graphene. Nanodevices can create ultrasensitive sensors and can be designed with spatial resolution as fine as the subcellular regime. Structures on the nanoscale can enable the development of engineered tissues within which sensing elements are integrated as closely as the nervous system within native tissues. In addition, the close integration of nanomaterials with cells and tissues will also allow the development of in vitro platforms for basic research or diagnostics. Such lab-on-a-chip systems could, for example, enable testing of the effects of candidate therapeutic molecules on intercellular, single-cell, and even intracellular physiology. Finally, advances in nanoelectronics can lead to extremely sophisticated smart materials with multifunctional capabilities, enabling the spectrum of biomedical possibilities from diagnostic studies to the creation of cyborgs.

- Visibly Transparent Polymer Solar Cells Produced by Solution Processing
  Chen, C.-C.; Dou, L.; Zhu, R.; Chung, C.-H.; Song, T.-B.; Zheng, Y. B.; Hawks, S.; Li, G.; Weiss, P. S.; Yang, Y. *ACS Nano* **2012**, *6*, 7185-7190.
  Abstract:

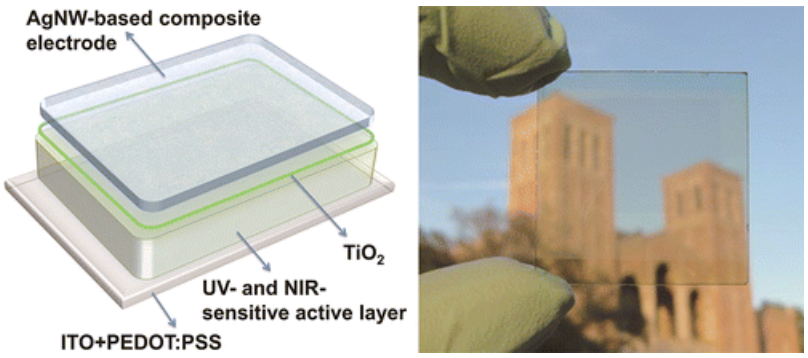

Visibly transparent photovoltaic devices can open photovoltaic applications in many areas, such as building-integrated photovoltaics or integrated photovoltaic chargers for portable electronics. We demonstrate high-performance, visibly transparent polymer solar cells fabricated via solution processing. The photoactive layer of these visibly transparent polymer solar cells harvests solar energy from the near-infrared region while being less sensitive to visible photons. The top transparent electrode employs a highly transparent silver nanowire–metal oxide composite conducting film, which is coated through mild solution processes. With this combination, we have achieved 4% power-conversion efficiency for solution-processed and visibly transparent polymer solar cells. The optimized devices have a maximum transparency of 66% at 550 nm.

- Progress in the Understanding of the Key Pharmacophoric Features of the Antimalarial Drug Dihydroartemisinin: An Experimental and Theoretical Charge Density Study
  Saleh, G.; Soave, R.; Lo Presti, L.; Destro, R. *Chem. Eur. J.* **2013**, *19*, 3490–3503.
  Abstract:

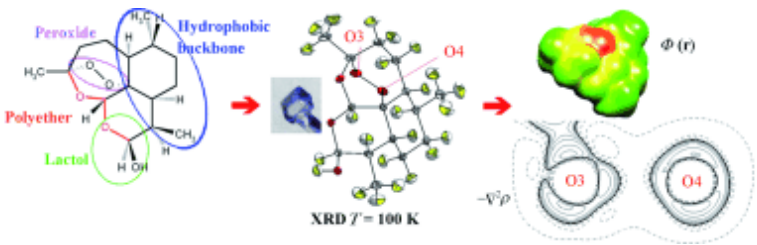

The accurate, experimental charge density distribution, $\rho(\mathbf{r})$, of the potent antimalarial drug dihydroartemisinin (DHA) has been derived for the first time from single-crystal X-ray diffraction data at T=100(2) K. Gas-phase and solid-state DFT simulations have also been performed to provide a firm basis of comparison with experimental results. The quantum theory of atoms in molecules (QTAIM) has been employed to analyse the $\rho(\mathbf{r})$ scalar field, with the aim of classifying and quantifying the key real-space elements responsible for the known pharmacophoric features of DHA. From the conformational perspective, the bicyclo[3.2.2]nonane system fixes the three-dimensional arrangement of the 1,2,4-trioxane bearing the active O=O redox centre. This is the most nucleophilic function in DHA and acts as an important CH···O acceptor. On the contrary, the rest of the molecular backbone is almost neutral, in accordance with the lipophilic character of the compound. Another remarkable feature is the C=O bond length alternation along the O-C-O-C polyether chain, due to correlations between pairs of adjacent C=O bonds. These bonding features have been related with possible reactivity routes of the α- and β-DHA epimers, namely 1) the base-catalysed hemiacetal breakdown and 2) the peroxide reduction. As a general conclusion, the base-driven proton transfer has significant non-local effects on the whole polyether chain, whereas DHA reduction is thermodynamically favourable and invariably leads to a significant weakening (or even breaking) of the O=O bond. The influence of the hemiacetal stereochemistry on the electronic properties of the system has also been considered. Such findings are discussed in the context of the known chemical reactivity of this class of important antimalarial drugs.

- Size-Selective Encapsulation of Hydrophobic Guests by Self-Assembled M_4L_6 Cobalt and Nickel Cages
  Ronson, T. K.; Giri, C.; Kodiah Beyeh, N.; Minkkinen, A.; Topić, F.; Holstein, J. J.; Rissanen, K.; Nitschke, J. R. *Chem. Eur. J.* **2013**, *19*, 3374–3382.
  Abstract:

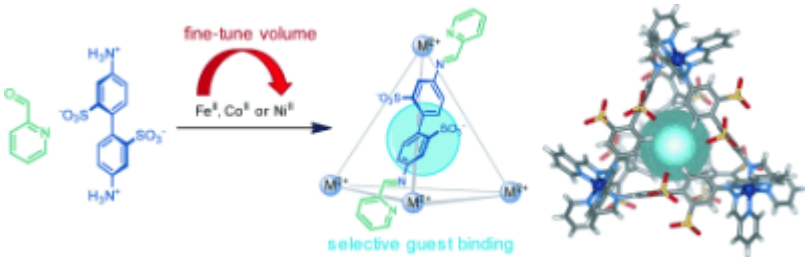

Subtle differences in metal–ligand bond lengths between a series of $[M_4L_6]^{4-}$ tetrahedral cages, where M=Fe^{II}, Co^{II}, or Ni^{II}, were observed to result in substantial differences in affinity for hydrophobic guests in water. Changing the metal ion from iron(II) to cobalt(II) or nickel(II) increases the size of the interior cavity of the cage and allows encapsulation of larger guest molecules. NMR spectroscopy was used to study the recognition properties of the iron(II) and cobalt(II) cages towards small hydrophobic guests in water, and single-crystal X-ray diffraction was used to study the solid-state complexes of the iron(II) and nickel(II) cages.

- Fluorescent Proteins: Shine on, You Crazy Diamond
  Dedecker, P.; De Schryver, F. C.; Hofkens, J. *J. Am. Chem. Soc.* **2013**, *135*, 2387–2402.
  Abstract:

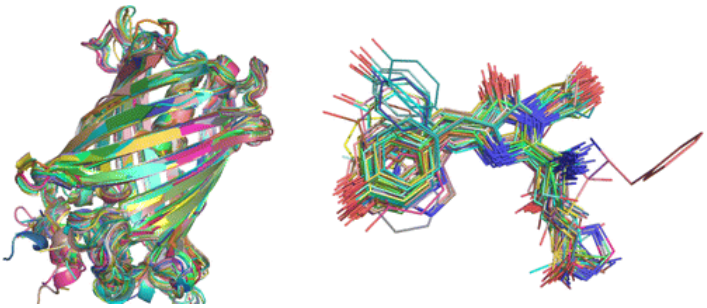

In this Perspective we discuss recent trends in the development and applications of fluorescent proteins. We start by providing a historical and structural perspective of their spectroscopic and structural aspects and describe how these properties have made fluorescent proteins essential as ‘smart labels’ for biosensing and advanced fluorescence imaging. We show that the strong link between the spectroscopic properties and protein structure and properties is a necessary element in these developments and that this dependence makes the proteins excellent model systems for a variety of fields. We pay particular attention to emerging or future research opportunities and unsolved questions.

- Efficient Self-Assembly in Water of Long Noncovalent Polymers by Nucleobase Analogues
  Cafferty, B. J.; Gállego, I.; Chen, M. C.; Farley, K. I.; Eritja, R.; Hud, N. V. *J. Am. Chem. Soc.* **2013**, *135,* 2207–2212.
  Abstract:

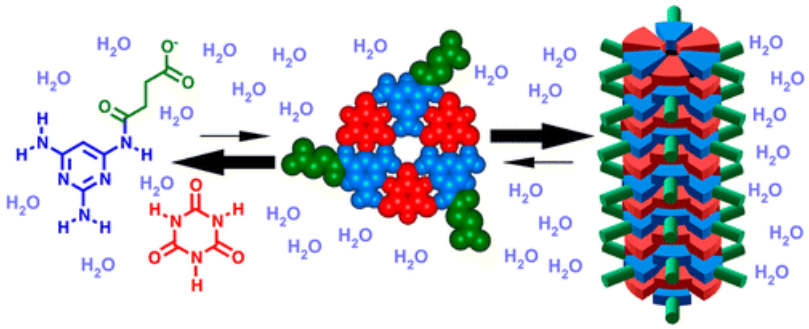

Molecular self-assembly is widely appreciated to result from a delicate balance between several noncovalent interactions and solvation effects. However, current design approaches for achieving self-assembly in water with small, synthetic molecules do not consider all aspects of the hydrophobic effect, in particular the requirement of surface areas greater than 1 nm2 for an appreciable free energy of hydration. With the concept of a minimum hydrophobic surface area in mind, we designed a system that achieves highly cooperative self-assembly in water. Two weakly interacting low-molecular-weight monomers (cyanuric acid and a modified triaminopyrimidine) are shown to form extremely long supramolecular polymer assemblies that retain water solubility. The complete absence of intermediate assemblies means that the observed equilibrium is between free monomers and supramolecular assemblies. These observations are in excellent agreement with literature values for the free energy of nucleic acid base interactions as well as the calculated free energy penalty for the exposure of hydrophobic structures in water. The results of our study have implications for the design of new self-assembling structures and hydrogel-forming molecules and may provide insights into the origin of the first RNA-like polymers.

- Molecular Imprinting of Luminescent Vesicles
  Banerjee, S.; König, B. *J. Am. Chem. Soc.* **2013**, *135*, 2967–2970.

Abstract:

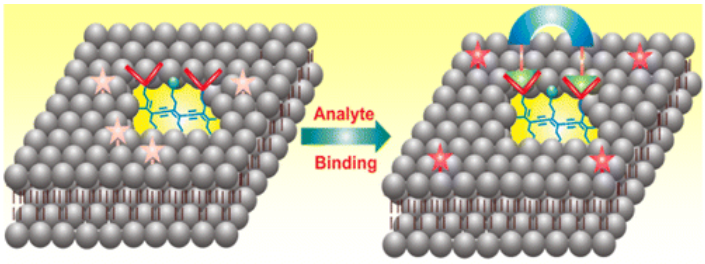

Applying molecular imprinting techniques to the surface of functionalized unilammelar fluid vesicles allows the preparation of specific and high-affinity luminescent chemosensors. We have photopolymerized diacetylene containing vesicles in the presence of small peptides as templates yielding imprinted polydiacetylene (PDA) patches in the membrane. They serve as multivalent receptor sites with significantly increased rebinding affinity for the template. All binding sites are surface exposed and accessible for analyte binding. The presence of analytes is signaled with high sensitivity by emission intensity changes of amphiphilic carboxyfluorescein, which is coembedded into the fluid DOPC membrane. The merger of PDA imprinting with dynamic functionalized vesicles overcomes some of the current limitations of molecular imprinting in chemosensor design and may be applied to many different target analytes.

- Supramolecular Nanostructures Formed by Anticancer Drug Assembly
  Cheetham, A. G.; Zhang, P.; Lin, Y.-A.; Lock, L. L.; Cui, H. *J. Am. Chem. Soc.* **2013**, *135*, 2907–2910.
  Abstract:

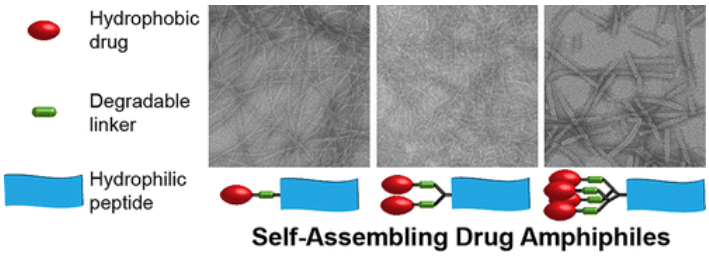

We report here a supramolecular strategy to directly assemble the small molecular hydrophobic anticancer drug camptothecin (CPT) into discrete, stable, well-defined nanostructures with a high and quantitative drug loading. Depending on the number of CPTs in the molecular design, the resulting nanostructures can be either nanofibers or nanotubes, and have a fixed CPT loading content ranging from 23% to 38%. We found that formation of nanostructures provides protection for both the CPT drug and the biodegradable linker from the external environment and thus offers a mechanism for controlled release of CPT. Under tumor-relevant conditions, these drug nanostructures can release the bioactive form of CPT and show in vitro efficacy against a number of cancer cell lines. This strategy can be extended to construct nanostructures of other types of anticancer drugs and thus presents new opportunities for the development of self-delivering drugs for cancer therapeutics.

- Gold nanoparticles with flexible mesogenic grafting layers
  Wolska, J. M.; Pociecha, D.; Mieczkowski, J.; Gorecka, E. *Soft Matter* **2013,** *9*, 3005-3008.
  Abstract:

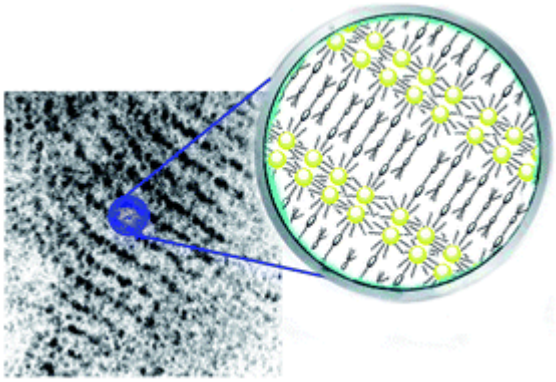

Self-organization of gold nanoparticles depends strongly on their organic coating. Lamellar structures were obtained by using double grafting – small Au nanoparticles were covered with *n*-alkyl thiol molecules and further with monomeric or dimeric type mesogenic molecules. Apart from positional correlations of metallic centres the structures also showed orientational order of mesogenic ligands manifested as optical birefringence.

- The leverage effect of the relative strength of molecular solvophobicity vs. solvophilicity on fine-tuning nanomorphologies of perylene diimide bolaamphiphiles
  Zhang, Z.; Zhang, X.; Zhan, C.; Lu, Z.; Ding, X.; He, S.; Yao, J. *Soft Matter* **2013,** *9*, 3089-3097.
  Abstract:

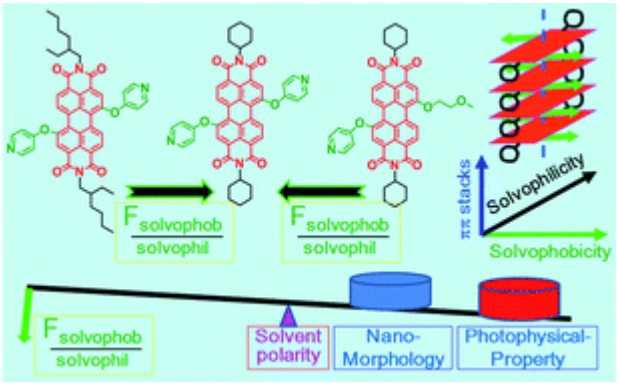

Previously, we have found that full protonation of the two pyridyloxyl groups of 1,7-bispyridyloxyl-*N*,*N*′-bis(2-ethylhexyl)perylene diimide (PDI) (molecule **1**) leads to formation of highly fluorescent nanospheres, due to formation of 1,7-bis(4-oxylpyridinium chloride) dramatically enhancing the inter-chromophore interactions in the bay-region (*J. Am. Chem. Soc.*, 2011, **133**, 11022–11025; *Chem.–Eur. J.*, 2012, **18**, 12305–12313). Molecular modeling revealed that the two pyridyloxyl groups in molecule **1** pointed outside the same facet of the PDI plane, forming a rigid PDI-based bolaamphiphile. In order to more fully investigate the effects of the molecular *solvophob*icity on the bay-region *vs.* the molecular *solvophil*icity including that from the imide-direction and from the solvophilic PDI unit, $F_{solvophob/solvophil}$, on fine-tuning nanomorphologies and properties, we reduced the molecular solvophilicity by replacing the two 2-ethylhexyl (EH) tails in molecule **1** with two shorter cyclohexyl (CH) tails, while maintaining the two 1,7-bispyridyloxyl units, forming molecule **2**. Furthermore, we replaced one pyridyloxyl group in molecule **2** with another weaker solvophobic 2-methoxyethoxyl unit, forming molecule **3** to tune the molecular solvophobicity in the bay-region. Morphological studies demonstrated that molecule **2** formed 70–400 nm sized hollow nanospheres in a polar solvent mixture of dichloromethane (DCM)–ethanol (EtOH) and ~100 nm sized hollow nanoparticles in a weak apolar environment of DCM–methylcyclohexane (MCH) mixture with R_{MCH} = 10–40% (v/v).

Upon a further increase of the surrounding apolarity by increasing the R_{MCH}, plate morphologies of nanorods and microplates formed, accompanying with the π–π-stacking changing from the co-facial mode to slippage mode. Differently, molecule **3** always formed platelike nanostructures such as nanotapes in DCM–EtOH mixtures and nano-rhombuses in DCM–MCH mixtures with the molecules adopting co-facial π–π-stacking in both nanostructures. Taken together, the self-assembly and the final nanomorphologies of the PDI-based bolaamphiphiles are both significantly controlled by a small change of $F_{solvophob/solvophil}$ and such a leverage effect of the control from $F_{solvophob/solvophil}$ is amplified by changing the solvent polarity, for example, fine-tuning R_{EtOH} and R_{MCH}.

- Is the special pair structure a good strategy for the kinetics during the last step of the energy transfer with the nearest antenna? A chemical model approach
  Camus, J. M.; Langlois, A.; Aly, S. M.; Guilard, R.; Harvey, P. D. *Chem. Commun.* **2013**, *49*, 2228-2230.
  Abstract:

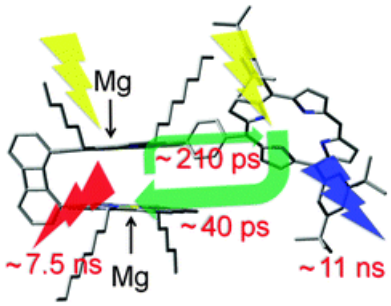

A cofacial bis(Mg(II)porphyrin)–C_6H_4-free base ([Mg_2]–bridge–FB) dyad shows S_1 energy transfer in both directions and much slower rates than similar monoporphyrin systems are observed.

- Chirality transcription and amplification by [2]pseudorotaxanes
  Kuwahara, S.; Chamura, R.; Tsuchiya, S.; Ikeda, M.; Habata, Y. *Chem. Commun.* **2013**, *49*, 2186-2188.
  Abstract:

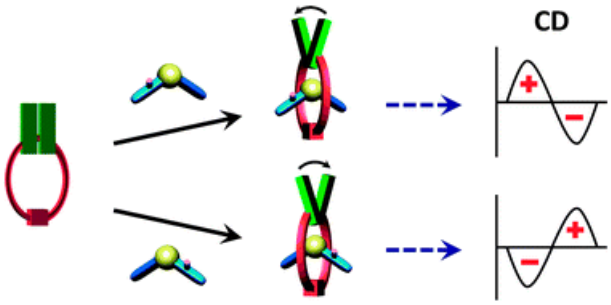

Chirality transcription and amplification by the formation of chiral [2]pseudorotaxanes by an achiral crown ether having the 2′,2″-quaterphenyl group and chiral sec-ammonium ions are reported. It was revealed that the absolute configurations of the chiral sec-ammonium ions can be detected directly from the CD spectra of the chiral [2]pseudorotaxanes.

- Charged and metallic molecular monolayers through surface-induced aromatic stabilization
  Heimel, G.; Duhm, S.; Salzmann, I.; Gerlach, A.; Strozecka, A.; Niederhausen, J.; Bürker, C.; Hosokai, T.; Fernandez-Torrente, I.; Schulze, G.; Winkler, S.; Wilke, A.; Schlesinger, R.;

Frisch, J.; Bröker, B.; Vollmer, A.; Detlefs, B.; Pflaum, J.; Kera, S.; Franke, K. J.; Ueno, N.; Pascual, J. I.; Schreiber, F.; Koch, N. *Nature Chemistry* **2013**, *5*, 187–194.

Abstract:

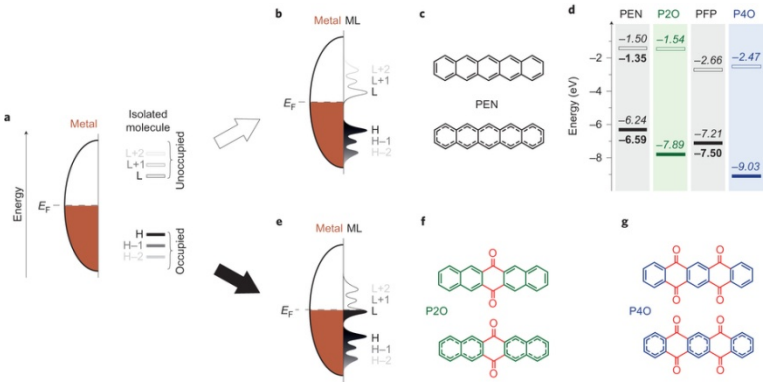

Large π-conjugated molecules, when in contact with a metal surface, usually retain a finite electronic gap and, in this sense, stay semiconducting. In some cases, however, the metallic character of the underlying substrate is seen to extend onto the first molecular layer. Here, we develop a chemical rationale for this intriguing phenomenon. In many reported instances, we find that the conjugation length of the organic semiconductors increases significantly through the bonding of specific substituents to the metal surface and through the concomitant rehybridization of the entire backbone structure. The molecules at the interface are thus converted into different chemical species with a strongly reduced electronic gap. This mechanism of surface-induced aromatic stabilization helps molecules to overcome competing phenomena that tend to keep the metal Fermi level between their frontier orbitals. Our findings aid in the design of stable precursors for metallic molecular monolayers, and thus enable new routes for the chemical engineering of metal surfaces.

- Vertically stacked multi-heterostructures of layered materials for logic transistors and complementary inverters

  Yu, W. J.; Li, Z.; Zhou, H.; Chen, Y.; Wang, Y.; Huang, Y.; Duan, X. *Nature Materials* **2013**, *12*, 246–252.

  Abstract:

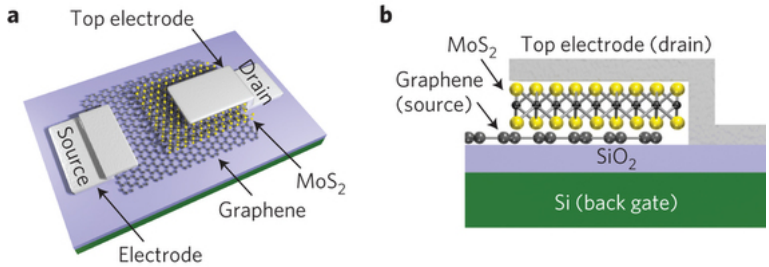

Graphene has attracted considerable interest for future electronics, but the absence of a bandgap limits its direct applicability in transistors and logic devices. Recently, other layered materials such as molybdenum disulphide (MoS_2) have been investigated to address this challenge. Here, we report the vertical integration of multi-heterostructures of layered materials for the fabrication of a new generation of vertical field-effect transistors (VFETs) with a room temperature on–off ratio > 10^3 and a high current density of up to 5,000 A cm^{-2}. An n-channel VFET is created by sandwiching few-layer MoS_2 as the semiconducting channel between a monolayer graphene sheet and a metal thin film. This approach offers a general strategy for the vertical integration of p- and n-channel transistors for high-performance logic applications. As an example, we demonstrate a complementary inverter

with a larger-than-unity voltage gain by vertically stacking graphene, $Bi_2Sr_2Co_2O_8$ (p-channel), graphene, MoS_2 (n-channel) and a metal thin film in sequence. The ability to simultaneously achieve a high on–off ratio, a high current density and a logic function in such vertically stacked multi-heterostructures can open up possibilities for three-dimensional integration in future electronics.

- Tuning Optical Properties of Si Quantum Dots by π-Conjugated Capping Molecules
  Dung, M. X.; Tung, D. D.; Jeong, S.; Jeong, H.-D. *Chem. Asian J.* **2013***, 8, 6*53-664.
  Abstract:

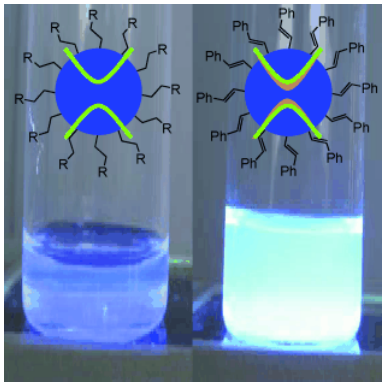

The absorption and photoluminescence (PL) properties of silicon quantum dots (QDs) are greatly influenced by their size and surface chemistry. Herein, we examined the optical properties of three Si QDs with increasing σ–π conjugation length: octyl-, (trimethylsilyl)vinyl-, and 2-phenylvinyl-capped Si QDs. The PL photon energy obtained from as-prepared samples decreased by 0.1–0.3 eV, while the PL excitation (PLE) extended from 360 nm (octyl-capped Si QDs) to 400 nm (2-phenylvinyl-capped Si QDs). A vibrational PL feature was observed in all samples with an energy separation of about 0.192±0.013 eV, which was explained based on electron–phonon coupling. After soft oxidization through drying, all samples showed blue PL with maxima at approximately 410 nm. A similar high-energy peak was observed with the bare Si QD sample. The changes in the optical properties of Si QDs were mainly explained by the formation of additional states arising from the strong σ–π conjugation and QD oxidation.

- Synthesis, Physical Properties, and Self-Assembly of A Novel Asymmetric Aroyleneimidazophenazine
  Zhao, J.; Wong, J. I.; Wang, C.; Gao, J.; Ng, V. Z. Y.; Yang, H. Y.; Loo, S. C. J.; Zhang, Q. *Chem. Asian J.* **2013***, 8,* 665-669.
  Abstract:

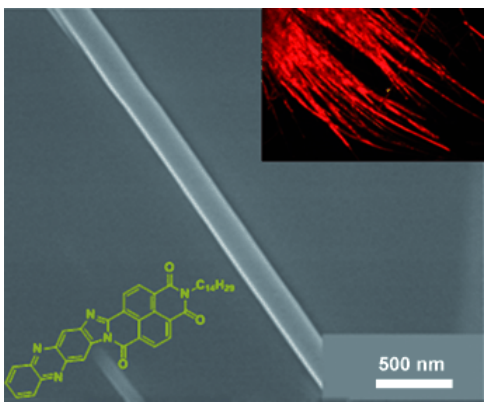

The synthesis, physical properties, and self-assembly of a novel asymmetric

aroyleneimidazophenazine (IZ1) is reported. The as-prepared IZ1 nanowires display an obvious red fluorescence. A heterojunction light-emitting diode (LED) device with the structure ITO/IZ1 nanowires/p-SiC/Al (10 nm)/Ti (80 nm)/Al (380 nm)/ITO was fabricated, and electroluminescence emission with two peaks at about 412 nm and 613 nm was detected with a forward bias ranging from 5 to 10 V.

- The Pnicogen Bond: Its Relation to Hydrogen, Halogen, and Other Noncovalent Bonds
  Scheiner, S. *Acc. Chem. Res.* **2013**, *46*, 280–288.
  Abstract:

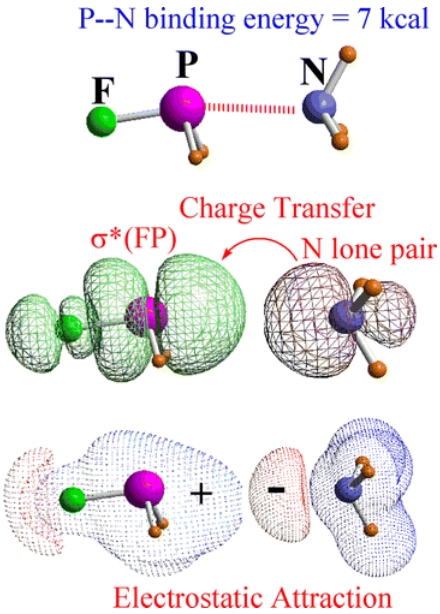

Among a wide range of noncovalent interactions, hydrogen (H) bonds are well known for their specific roles in various chemical and biological phenomena. When describing conventional hydrogen bonding, researchers use the notation AH···D (where A refers to the electron acceptor and D to the donor). However, the AH molecule engaged in a AH···D H-bond can also be pivoted around by roughly 180°, resulting in a HA···D arrangement. Even without the H atom in a bridging position, this arrangement can be attractive, as explained in this Account. The electron density donated by D transfers into a AH σ* antibonding orbital in either case: the lobe of the σ* orbital near the H atom in the H-bonding AH···D geometry, or the lobe proximate to the A atom in the HA···D case. A favorable electrostatic interaction energy between the two molecules supplements this charge transfer. When A belongs to the pnictide family of elements, which include phosphorus, arsenic, antimony, and bismuth, this type of interaction is called a pnicogen bond. This bonding interaction is somewhat analogous to the chalcogen and halogen bonds that arise when A is an element in group 16 or 17, respectively, of the periodic table.

Electronegative substitutions, such as a F for a H atom opposite the electron donor atom, strengthen the pnicogen bond. For example, the binding energy in $FH_2P\cdots NH_3$ greatly exceeds that of the paradigmatic H-bonding water dimer. Surprisingly, di- or tri-halogenation does not produce any additional stabilization, in marked contrast to H-bonds. Chalcogen and halogen bonds show similar strength to the pnicogen bond for a given electron-withdrawing substituent. This insensitivity to the electron-acceptor atom distinguishes these interactions from H-bonds, in which energy depends strongly upon the identity of the proton-donor atom.

As with H-bonds, pnicogen bonds can extract electron density from the lone pairs of atoms on the

partner molecule, such as N, O, and S. The π systems of carbon chains can donate electron density in pnicogen bonds. Indeed, the strength of A···π pnicogen bonds exceeds that of H-bonds even when using strong proton donors such as water with the same π system.

H-bonds typically have a high propensity for a linear AH···D arrangement, but pnicogen bonds show an even greater degree of anisotropy. Distortions of pnicogen bonds away from their preferred geometry cause a more rapid loss of stability than in H-bonds. Although often observed in dimers in the gas phase, pnicogen bonds also serve as the glue in larger aggregates, and researchers have found them in a number of diffraction studies of crystals.

- Control of Charge Transfer in Donor/Acceptor Metal–Organic Frameworks
  Miyasaka, H. *Acc. Chem. Res.* **2013**, *46*, 248–257.
  Abstract:

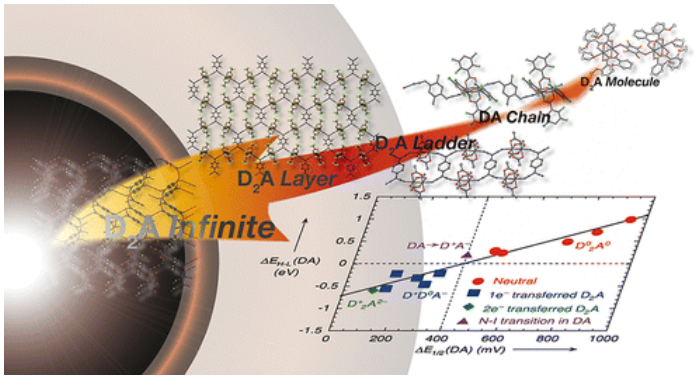

Charge transfer (CT) of $D^0A^0 \leftrightarrow D^{\delta+}A^{\delta-}$ not only involves an electron transfer from D to A, but also generates a new spin set of $S = 1/2$ spins with an exchange interaction. Therefore, the control of CT in multidimensional frameworks could be an efficient way to design electronically/magnetically functional materials. The use of redox-active metal complexes as D and/or A building blocks expands the variety of such D/A frameworks with the formulation of D_mA_n (m, $n \geq 1$), permitting the design of donor/acceptor metal–organic frameworks (D/A-MOFs). This Account summarizes our ongoing research on the design of D/A-MOFs and on the systematic control of CT in such D/A-MOFs toward the discovery of unique electronic/magnetic materials exhibiting nontrivial phenomena. For this purpose, the D/A combinations of carboxylate-bridged paddlewheel-type diruthenium(II,II) complexes ($[Ru_2^{II,II}]$) that act as one-electron ($1e^-$) donors and polycyanoorganic acceptors such as 7,7,8,8-tetracyano-*p*-quinodimethane (TCNQ) and *N*,*N*′-dicyanoquinodiimine (DCNQI) have been chosen.

Even in the covalently bonded motif, the CT in this system is systematically dependent on the intrinsic ionization potential (I_D) and electron affinity (E_A) of the D and A units, respectively, which is controllable by chemical modification of the D/A units. As we consider the energy difference between the HOMO of D and the LUMO of A ($\Delta E_{H\text{-}L}(DA)$) instead of $h\nu_{CT} \propto |I_D - E_A|$, the neutral (N) and ionic (I) states can be defined as follows: (i) the D/A materials with $\Delta E_{H\text{-}L}(DA) > 0$ (i.e., the LUMO level of A is higher than the HOMO level of D) should be neutral, and (ii) complexes adopted when $\Delta E_{H\text{-}L}(DA) < 0$ are, meanwhile, ionic. Materials located near $\Delta E_{H\text{-}L}(DA) \approx 0$, that is, at the boundary between the N and I phases, are candidates for the N–I transition driven by external stimuli such as temperature, pressure, and photoirradiation. Even in the ionic state, two distinct states could be isolated for the D_2A type: (ii-1) the $1e^-$ transferred D_2A-MOFs provide mixed-valence systems of $D^+D^0A^-$ possibly involving intervalence CT, which produce magnetic correlations via radical A^- units, and (ii-2) when the $2e^-$ reduced form of A (e.g., $TCNQ^{2-}$) is energetically favored beyond the on-site Coulomb

repulsion on A, the oxidation state of $D^{+}{}_{2}A^{2-}$ is produced, for which magnetic measurements reveal a paramagnetic state attributed to the isolated D^{+} units.

The interspatial Coulombic interaction is another factor in determining the charge distribution in materials, which is related to the spatial Coulombic stability of D/A packing and possibly yields a mixture of N and I domains when it is more advantageous to get Coulombic gain than in the uniform N or I phase. Such a phase could be observed at the boundary between N and I phases involving the N–I transition.

These charge-distributed states/phases are systematically demonstrated in a D/A-MOF system made by the combination of $[Ru_2^{II,II}]$ and TCNQ/DCNQI; however, we immediately recognize the charge distribution of D/A-MOF only by understanding the nature of the starting D/A units. The present D/A-MOF system should be an intriguing platform to look for new functionalities with synergistic correlations among charge, spin, and lattice.

- Chirally Homogeneous and Heterogeneous Dendritic Liquid Crystals
  Belaissaoui, A.; Saez, I. M.; Cowling, S. J.; Goodby, J. W. *Macromolecules* **2013**, *46*, 1268-1273.
  Abstract:

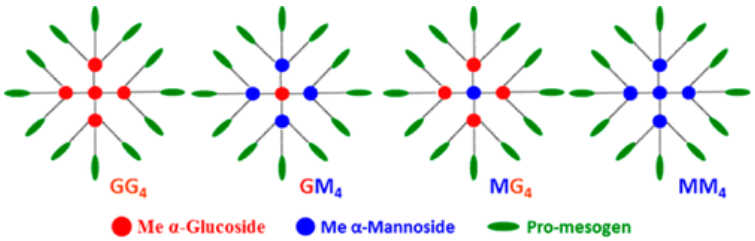

We have coupled methyl α-d-glucoside (G) and methyl α-d-mannoside (M) as the chiral structural variant moieties in the core and at the branching sites within dendritic scaffolds surrounded by 12 cyanobiphenyl mesogens (CB). Systematic studies of the influence of the chiral moieties on thermal and mesomorphic properties were carried out by positional permutation approach of the pyranose units G and M within the core and branching points. The mesomorphic properties of the chirally homogeneous dendrimers GG4/MM4 and the corresponding chirally heterogeneous dendritic homologues GM4/MG4 were investigated by differential scanning calorimetry (DSC) and polarized optical microscopy (POM). Remarkably, the thermal profile and the mesophase structure of the four dendrimers appear to be significantly independent of the nature of the central chiral core. The outer chirality at the periphery significantly dominates the liquid crystalline properties.

- Facile Syntheses of Cucurbit[6]uril-Anchored Polymers and Their Noncovalent Modification
  Huang, X.; Hu, F.; Su, H. *Macromolecules* **2013**, *46*, 1274-1282.
  Abstract:

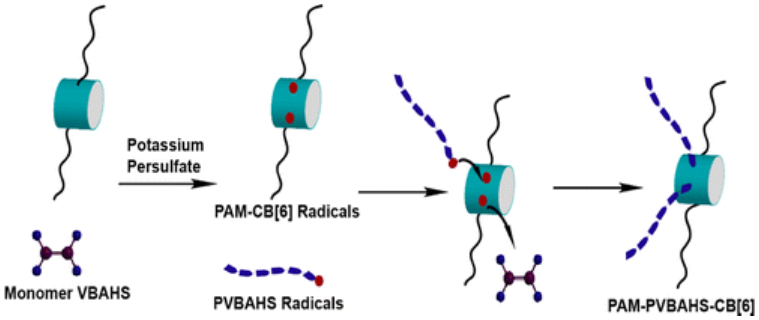

The general strategy for facile synthesis of Cucurbit[6]uril- (CB[6]-) anchored polymers without the

functionalization of CB[6] was presented. The acrylamide as a typical monomer was used to synthesize a series of CB[6]-anchored polyacrylamides (CB[6]-PAM) using potassium persulfateas as initiator and oxidant. The CB[6]-PAM samples were characterized by ^{1}H NMR, ^{13}C NMR, HMQC, FTIR, and TGA. It was found that the composition and chain microstructure of CB[6]-PAM polymers could be tunable by changing the content of potassium persulfate, CB[6] and acrylamide. In addition, CB[6]-PAM could be assembled into nanosized vesicles, which were confirmed by TEM, AFM, and SEM measurements. By taking advantage of the exceptional binding affinity of the CB[6], the CB[6]-PAM could be modified with butyl amine hydrochloride. The result makes the CB[6]-anchored polymer potentially useful in many applications. Furthermore, this synthetic approach could be extend to CB[6]-anchored polymers with two different chains. As a typical example, CB[6]-anchored poly(4-vinylbenzylamine hydrochloride salt) and polyacrylamide was synthesized successfully.

- Materials Science and Materials Chemistry for Large Scale Electrochemical Energy Storage: From Transportation to Electrical Grid
  Liu, J.; Zhang, J.-G.; Yang, Z.; Lemmon, J. P.; Imhoff, C.; Graff, G. L.; Li, L.; Hu, J.; Wang, C.; Xiao, J.; Xia, G.; Viswanathan, V. V.; Baskaran, S.; Sprenkle, V.; Li, X.; Shao, Y.; Schwenzer, B. *Adv. Funct. Mater.* **2013**, *23*, 929–946.
  Abstract:

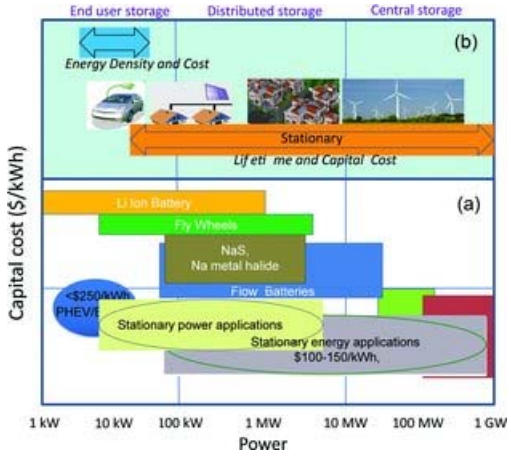

Large-scale electrical energy storage has become more important than ever for reducing fossil energy consumption in transportation and for the widespread deployment of intermittent renewable energy in electric grid. However, significant challenges exist for its applications. Here, the status and challenges are reviewed from the perspective of materials science and materials chemistry in electrochemical energy storage technologies, such as Li-ion batteries, sodium (sulfur and metal halide) batteries, Pb-acid battery, redox flow batteries, and supercapacitors. Perspectives and approaches are introduced for emerging battery designs and new chemistry combinations to reduce the cost of energy storage devices.

- ABAB-Symmetric Tetraalkyl Titanyl Phthalocyanines for Solution Processed Organic Field-Effect Transistors with Mobility Approaching 1 $cm^2 V^{-1} s^{-1}$
  Dong, S.; Bao, C.; Tian, H.; Yan, D; Geng, Y.; Wang, F. *Adv. Mater.* **2013**, *25*, 1165–1169.
  Abstract:

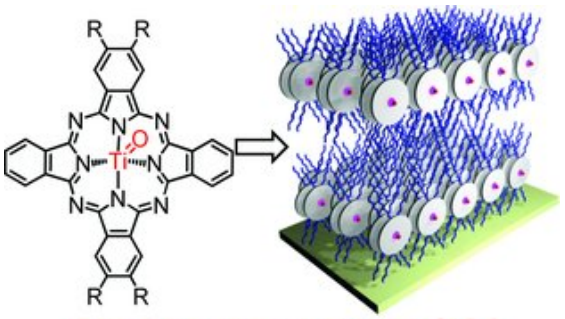

In crystals, tetraalkyl vanadyl phthalocyanines (OVPc-Cn) and tetraalkyl titanyl phthalocyanines (OTiPc-Cn) with ABAB symmetry adopt a 2D slipped π–π stacking motif with alkyl chains locating in the space between semiconducting layers formed by Pc cores. Hole mobility approaching 1 $cm^2\ V^{-1}\ s^{-1}$ is achieved for spin cast OFETs.

- Living Crystals of Light-Activated Colloidal Surfers
  Palacci, J.; Sacanna, S.; Preska Steinberg, A.; Pine, D. J.; Chaikin, P. M. *Science* **2013**, *339*, 936-940.
  Abstract:

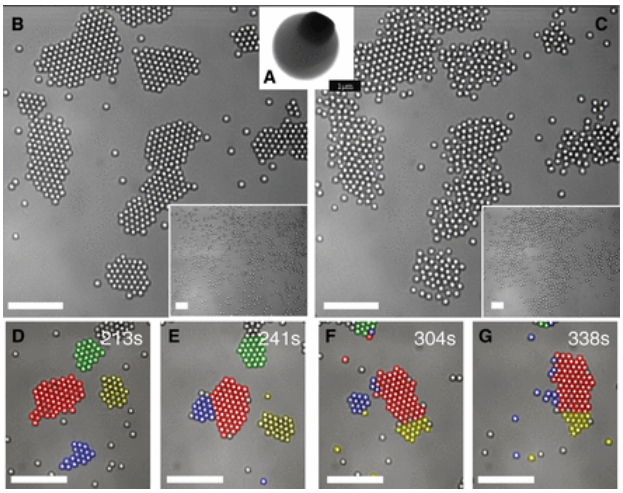

Spontaneous formation of colonies of bacteria or flocks of birds are examples of self-organization in active living matter. Here, we demonstrate a form of self-organization from nonequilibrium driving forces in a suspension of synthetic photoactivated colloidal particles. They lead to two-dimensional "living crystals," which form, break, explode, and re-form elsewhere. The dynamic assembly results from a competition between self-propulsion of particles and an attractive interaction induced respectively by osmotic and phoretic effects and activated by light. We measured a transition from normal to giant-number fluctuations. Our experiments are quantitatively described by simple numerical simulations. We show that the existence of the living crystals is intrinsically related to the out-of-equilibrium collisions of the self-propelled particles.

- Direct chemical evidence for sphingolipid domains in the plasma membranes of fibroblasts
  Frisz, J. F.; Lou, K.; Klitzing, H. A.; Hanafin, W. P.; Lizunov, V.; Wilson, R. L.; Carpenter, K. J.; Kim, R.; Hutcheon, I. D.; Zimmerberg, J.; Weber, P. K.; Kraft, M. L. *Proc. Nat. Acad. Sci. USA* **2013**, *110*, 613-622.
  Abstract:

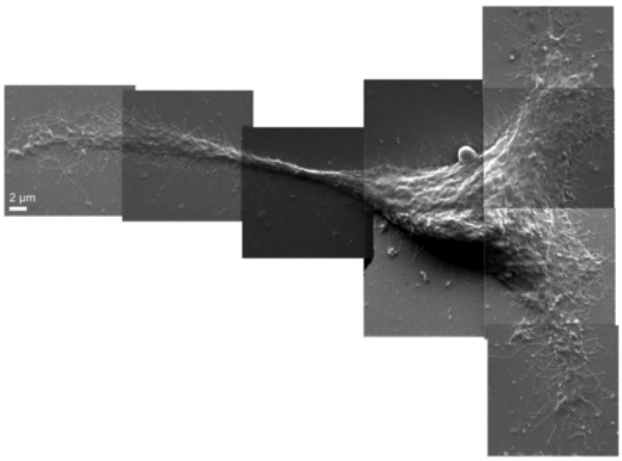

Sphingolipids play important roles in plasma membrane structure and cell signaling. However, their lateral distribution in the plasma membrane is poorly understood. Here we quantitatively analyzed the sphingolipid organization on the entire dorsal surface of intact cells by mapping the distribution of ^{15}N-enriched ions from metabolically labeled ^{15}N-sphingolipids in the plasma membrane, using high-resolution imaging mass spectrometry. Many types of control experiments (internal, positive, negative, and fixation temperature), along with parallel experiments involving the imaging of fluorescent sphingolipids—both in living cells and during fixation of living cells—exclude potential artifacts. Micrometer-scale sphingolipid patches consisting of numerous ^{15}N-sphingolipid microdomains with mean diameters of ~200 nm are always present in the plasma membrane. Depletion of 30% of the cellular cholesterol did not eliminate the sphingolipid domains, but did reduce their abundance and long-range organization in the plasma membrane. In contrast, disruption of the cytoskeleton eliminated the sphingolipid domains. These results indicate that these sphingolipid assemblages are not lipid rafts and are instead a distinctly different type of sphingolipid-enriched plasma membrane domain that depends upon cortical actin.

- Molecular Self-Assembly: Smart Design of Surface and Interface via Secondary Molecular Interactions
  Lee, I. *Langmuir* **2013**, *29*, 2476–2489.
  Abstract:

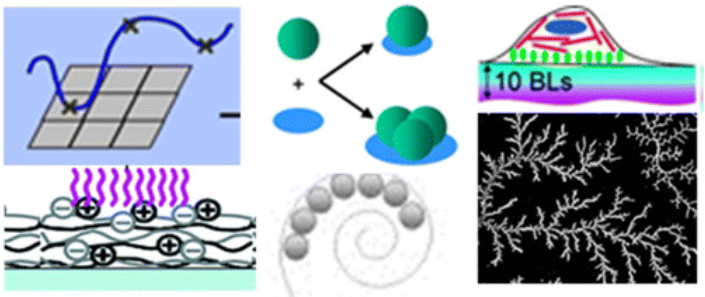

The molecular self-assembly of macromolecular species such as polymers, colloids, nano/microparticles, proteins, and cells when they interface with a solid/substrate surface has been studied for many years, especially in terms of molecular interactions, adsorption, and adhesion. Such fundamental knowledge is practically important in designing smart micro- and nanodevices and sensors, including biologically implantable ones. This review gives a brief sketch of molecular self-assembly and nanostructured multifunctional thin films that utilize secondary molecular interactions at surfaces and interfaces.

- A Fluorescent Organic Nanotube Assembled from Novel p-Phenylene Ethynylene-Based Dicationic Amphiphiles
  Chen, A.-J.; Hsu, I.-J.; Wu, W.-Y.; Su, Y.-T.; Tsai, F.-Y.; Mou, C.-Y. *Langmuir* **2013**, *29*, 2580–2587.
  Abstract:

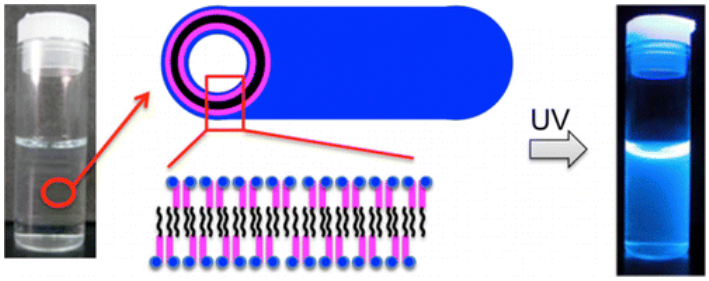

Novel π–extended conjugated amphiphiles composed of a hydrophilic section of two quaternary ammonium groups and p-phenylene ethynylene with adjustable alkyl chain hydrophobic section were prepared by a multistep synthesis. These dicationic amphiphiles showed good water solubility and formed a tubular assembly in water. The evidence for the nanotubular comes from direct optical and TEM observations. A strong π–π stacking interaction between neighboring molecules, as evidenced by the red-shift and self-quenching in fluorescence, is proposed for the self-assembly. At the same time, dehydration of the bromide led to strong counterion condensation in headgroups, which resulted in the small curvature structure of the nanotubes. A bilayer lamellar structural model for the organic nanotube is proposed, and a reasonable structural model based on the experimental XRD pattern, as well as cell constants, is proposed.